

Self-assembly of three-dimensional photonic-crystals with air-core line defects

Yong-Hong Ye,* Theresa S. Mayer, Iam-Choon Khoo, Ivan B. Divliansky, Neal Abrams and Thomas E. Mallouk

Center for Collective Phenomena in Restricted Geometries, The Pennsylvania State University, University Park, PA 16802, USA

Received 30th July 2002, Accepted 30th August 2002

First published as an Advance Article on the web 4th October 2002

We have introduced line defects into a three-dimensional (3D) photonic crystal by combining the techniques of optical photolithography, self-assembly, and template replication. The template is a colloidal crystal film that is grown on a silicon or glass substrate patterned with photoresist lines, and the 3D photonic crystal with air-core line defects is obtained by infiltrating the colloidal crystal film with silica and removing the template by calcination. SEM and optical transmission spectra show that the resulting 3D PC structure has high structural integrity and crystalline quality. This approach can introduce defects at the desired places of 3D photonic crystals, which may be useful in making 3D photonic crystal-based air-core waveguides.

I Introduction

Photonic crystals (PCs) are a promising platform for the realization of integrated optoelectronic circuits.¹ Recently, there has been considerable interest in fabricating three-dimensional (3D) PCs and PC-based devices designed for optical wavelengths.^{2–4} A simple and inexpensive route by which to fabricate 3D PCs with a photonic bandgap of optical wavelength is through the self-assembly of colloidal microspheres.^{5–11} Though the currently available colloidal crystals do not have a full photonic bandgap because of their low index contrast, the self-assembled colloidal crystals provide an ideal template for the creation of porous structures with a full photonic bandgap by infiltration of the template by a material of high refractive index and then removal of the template.^{12–19} Most of the applications of PC based devices require exact placement of well-defined line or point defects in the interior of the PCs, which cannot be obtained through self-assembly alone. For example, if a line defect is introduced into a photonic crystal, a wavelength (λ)-scale optical waveguide can be fabricated, and such a PC waveguide can have unique properties, such as an arbitrary refractive index core, waveguiding through a λ -scale sharp bend, and extremely large group-velocity dispersion.^{20–22} Combination of the self-assembly approach with defect engineering is an important issue for making PC based devices. If intentional defects can be introduced into self-assembled colloidal crystals, it will be feasible to make PC-based devices using a self-assembly approach. However, few methods have been proposed to introduce defects at the desired places of colloidal crystals. Recently, Lee *et al.* demonstrated the multi-photo polymerization of 3D patterns in colloidal crystals by using a laser scanning confocal microscope.²³ Here, we show that air-core line defects can be introduced into inverse colloidal crystals by simply growing them on top of lithographically patterned substrates. SEM and optical transmission spectra measurements show that the resulting 3D PC structure has good crystalline quality.

II Experimental

Four steps were involved in the fabrication of the air-core line defects in 3D inverse colloidal crystals. (1) Standard photolithography was used to pattern the line structure on the

substrate. Both (001) p-type Si substrates and glass substrates were used. Samples fabricated on glass substrates were used for optical transmittance measurements. The line patterns were defined in a 1 μm thick layer of photoresist (Shipley 1811) that was spin coated on the substrate. The line patterns were 1 mm long. (2) A convective self-assembly method was used to grow colloidal crystals on the patterned substrates. The substrate was placed vertically into a vial containing an aqueous suspension of either 300 or 400 nm diameter polystyrene spheres. The volume fraction of the solution was around 0.5% wt. The vial is kept in a temperature-controlled oven. The drying process of the suspension ($\sim 5 \text{ mm day}^{-1}$) is observed from the top to the vial as water slowly evaporates from the aqueous colloidal solution. After completion of the drying process, an iridescent array of colloidal crystal film was deposited onto the substrate.^{8,9} The thickness (*i.e.* the number of layers) of the colloidal crystal was controlled by the concentration of the suspension. The resultant colloidal crystal film is of good quality, is stable in ethanol, and can be further inverted into macroporous SiO_2 film by using a sol-gel process, as demonstrated in our previous work.²⁴ (3) The photoresist lines on the substrate were removed by dipping the samples into ethanol for several minutes. During this step, the photoresist line arrays dissolved, leaving air cores surrounded by the colloidal crystal film. (4) The colloidal crystal film was further replicated to make an inverse opal structure. The voids in the colloidal crystal film were first infiltrated by silica *via* a modified sol-gel process involving the acid-catalyzed hydrolysis and condensation of an organic precursor, tetraethylorthosilicate (TEOS), in ethanol.^{24,25} A home-made dip-coating apparatus was used. The substrate containing the colloidal crystal with the air cores in the vertical direction was lowered into the precursor solution and then slowly withdrawn. Using this vertical dip-coating method, all the colloidal spheres, including the spheres surrounding the line defects, are coated with a very thin layer of silica sol,²⁴ leaving the line defects open. The sample was dried in air for 10 min. As a result of exposure to moisture in the air, the TEOS was hydrolyzed and most of the solvent in the precursor was removed, with the colloidal spheres being coated with a thin layer of silica gel. The cycle of infiltration, reaction, and drying was repeated several times until the voids in the colloidal crystal were completely filled with silica gel. Because the line defects are much bigger than the voids around the colloidal spheres, air cores appear at

the positions of the line defects, though their cross-sectional area exhibit a little shrinkage. The polystyrene spheres were then removed by calcination at 450 °C for 30 min. During this step, the polystyrene spheres decomposed, leaving behind air spheres in an SiO₂ matrix, as demonstrated in our previous work.²⁴

III Results and discussion

The 3D structures of the samples were characterized by a Philips XL20 W scanning electron microscope (SEM). Fig. 1 shows cross-sectional SEM images of the samples. Fig. 1(a) shows the patterned substrate. The photoresist pattern is periodic line arrays 1 μm high × 3 μm wide with 11 μm spacing. Fig. 1(b) shows the colloidal crystal multilayer film grown on the patterned substrate. The sphere size in this case was 400 nm. Fig. 1(b) shows that the photoresist lines are completely surrounded by 3D colloidal crystals. The polystyrene spheres are aligned into a face-centered cubic (FCC) close-packed lattice oriented in the (111) direction both in the channels between the photoresist lines and on the top surface of the photoresist lines. The plane normal to the photoresist lines is the (110) plane. Multilayered structures of up to 10 layers have exhibited excellent crystalline properties, and crystallized multilayers can be made up to 50 layers thick by increasing the concentration of the sphere suspension. Fig. 1(c) shows the 3D PC film after removing the photoresist lines. The cross-sectional image shows no sign of the photoresist lines. The resulting air cores keep the shape of the photoresist lines, and are surrounded by well-ordered 3D ordered colloidal crystals. The colloidal spheres do not collapse into the air channels until the channel width exceeds 4 μm. As the SEM is a cross-sectional image, the air-core structure shows that the photoresist lines were completely removed. Fig. 1(d) shows 3D photonic crystals with air-core line defects obtained after inversion of the crystal. The SEM image indicates that silica infiltration does not alter the width of the air channels surrounded by macroporous SiO₂, and there is little shrinkage in the lateral direction of the film. The size of the air spheres in the SiO₂ matrix exhibits shrinkage of ≤15% in the direction perpendicular to the substrate when compared with the polystyrene spheres, but the macroporous SiO₂ retains the 3D close-packed crystalline order of the initial template.

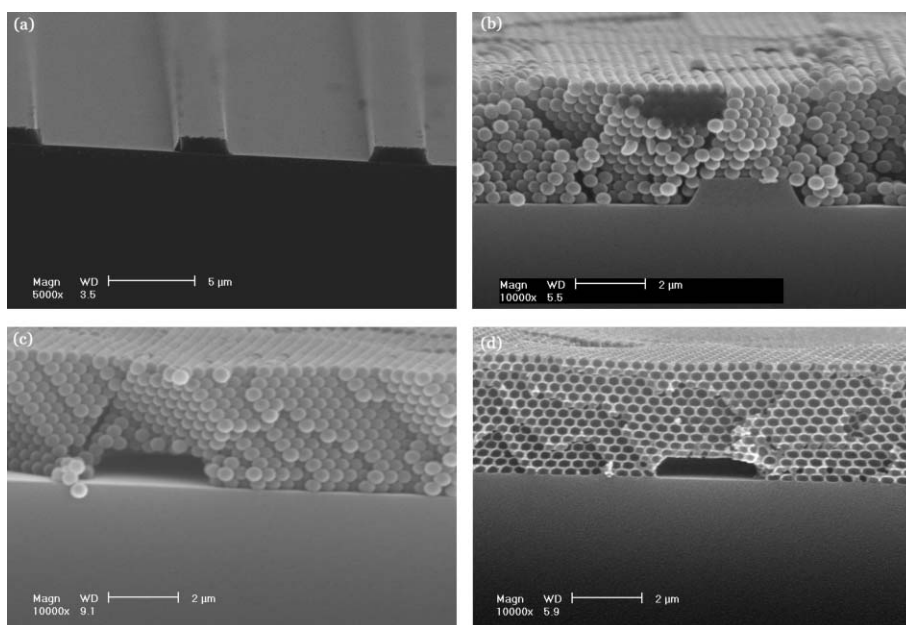


Fig. 1 (a) SEM image of the patterned substrate. The photoresist pattern is a periodic line array with 1 μm high × 3 μm wide lines, spaced at 11 μm. (b) SEM image of the patterned colloidal crystal multilayers, assembled using 0.4 μm polystyrene spheres. (c) SEM image of the patterned 3D colloidal crystal film after removing the photoresist lines. (d) SEM image of the air-core line defect embedded into inverse 3D colloidal crystals.

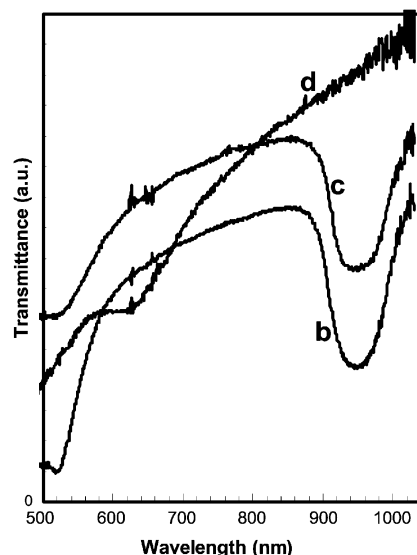


Fig. 2 Optical transmission spectra at normal incidence, where curves b, c, and d are spectra of the samples shown in Fig. 1(b), (c), and (d), respectively.

Fig. 2 shows optical transmission spectra at normal incidence, with curves b, c, and d obtained from macroscopic areas of the samples shown in Fig. 1(b), (c), and (d), respectively. The colloidal crystal multilayers show a clear stop band at 950 nm, which arises from the Bragg reflection of the (111) planes. The full width at half maximum (FWHM) is less than 10% of the center frequency of the band gap, as shown in curve b. The clear presence of the band gap confirms the high crystalline quality of the colloidal films inferred from the SEM images. The differences between spectra b and c may be due to removal of the photoresist lines, but the center position and FWHM of the stop band does not move because the removal of the photoresist lines does not damage the crystalline ordering of the structure. The crystalline ordering is still kept after the crystal is inverted by SiO₂ infiltration, so the macroporous SiO₂ film also exhibits a band gap. The central position of this band gap is shifted to 630 nm because of the change in the effective

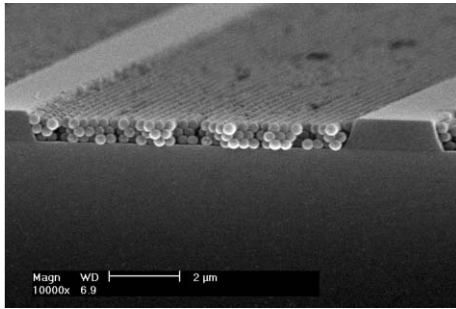


Fig. 3 SEM image of patterned colloidal crystal multilayers assembled using 0.3 μm polystyrene spheres at a concentration of 0.15 wt%.

refractive index of the structure and the shrinkage in the direction perpendicular to the film.

To explore the mechanism of the growth of colloidal crystals on patterned substrates, colloidal films were deposited onto substrates at a low concentration. Fig. 3 shows a cross-sectional SEM image of a sample. The concentration of the suspension in this case was about 0.15 wt%. Fig. 3 indicates that the growth of colloidal multilayers begins in the channels, which serve as physical traps for the polystyrene spheres. In particular, as the solvent evaporates from the surface of the substrate, a horizontally directed capillary force is induced on the spheres that are positioned on top of the photoresist lines. This force drives the spheres into the channels between the photoresist lines, where they assemble into a close-packed lattice due to immersion capillary interaction between adjacent spheres. After the channels are completely filled, the crystallization of polystyrene spheres will extend towards the top surfaces of the photoresist lines, as shown in Fig. 1. Stacking faults are minimized when the ratio of the height of the photoresist line to the sphere diameter is $1 + n(\frac{2}{3})^{0.5}$, where n is an integer. Previous work has revealed that substrate patterns have an effect on the symmetry of the colloidal arrays if the sphere size is comparable to the pattern spacing.^{26–30} In addition to hexagonal symmetry, centered rectangular symmetry can also occur. However, in this experiment, because the pattern spacing is large in comparison to the size of the polystyrene spheres, the substrate patterns have no effect on the symmetry of the colloidal crystalline films.

IV Conclusions

To summarize, by combining the colloidal crystal self-assembly technique and lithography, air-core line defects can be introduced at the desired places of 3D inverse colloidal crystals. Here, as an example, we report the fabrication of a silica photonic crystal with line defects. Moreover, we also find that this approach can yield colloidal crystal templates with line defects grown using $\sim 1 \mu\text{m}$ diameter polystyrene spheres, whose band gap is in the infrared region. Our next goal is to invert colloidal crystals with amorphous silicon (a-Si) to integrate an input coupler and an output coupler into the air-core structures, with a view to examining the efficiency of such a material as a waveguide. It has been demonstrated that colloidal templates can be filled with a-Si using low-pressure chemical vapor deposition (LPCVD) and plasma enhanced chemical vapor deposition.^{18,19} Due to its high refractive index contrast, a-Si PCs have full band gaps in the infrared region. If a substrate is pre-coated with a film of omnidirectional one-dimensional PCs with the same band gap as that of an inverted

a-Si PC, the air-core line defects fabricated in a-Si PCs can behave as waveguides, which means that this approach may be useful in making air-core waveguides in 3D PCs.

Acknowledgement

This research was supported by the NSF Material Research Science and Engineering Center, Collective Phenomena in Restricted Geometry, Grant DMR-0080019.

References

- 1 J. D. Joannopoulos, R. D. Meade and J. N. Winn, *Photonic Crystals*, Princeton University Press, Princeton, NJ, 1995;
- 2 E. Yablonovitch, *Phys. Rev. Lett.*, 1987, **58**, 2059; S. John, *Phys. Rev. Lett.*, 1987, **58**, 2486.
- 3 Y. Vlasov, V. Astratov, O. Karimov, A. Kaplyanskiy, V. Bogomolov and A. Prokofiev, *Phys. Rev. B*, 1997, **55**, R13357.
- 4 S. Lin, J. Fleming, M. Sigalas, R. Biswas and K. Ho, *Phys. Rev. B*, 1999, **59**, R15579.
- 5 M. Campbell, D. Sharp, M. Harrison, R. Denning and A. Turberfield, *Nature*, 2000, **404**, 53.
- 6 P. Pusey and W. Megen, *Nature*, 1986, **320**, 340.
- 7 I. Tarhan and G. Watson, *Phys. Rev. Lett.*, 1996, **76**, 315.
- 8 A. Blaaderen, R. Ruel and P. Wiltzius, *Nature*, 1997, **385**, 321.
- 9 N. D. Denkov, O. D. Velev, P. A. Kralchevsky, I. B. Ivanov, H. Yoshimura and K. Nagayama, *Nature*, 1993, **361**, 26.
- 10 P. Jiang, J. F. Bertone, K. S. Hwang and V. L. Colvin, *Chem. Mater.*, 1999, **11**, 2132.
- 11 Y. Xia, B. Gates, Y. Ying and Y. Lu, *Adv. Mater.*, 2000, **12**, 693.
- 12 D. McComb, B. Treble, C. Smith, R. M. De La Rue and N. Johnson, *J. Mater. Chem.*, 2001, **11**, 142.
- 13 C. Kresge, M. Leonowicz, W. Roth, J. Vartuli and J. Beck, *Nature*, 1992, **359**, 710.
- 14 O. Velev, T. Jede, R. Lobo and A. Lenhoff, *Nature*, 1997, **389**, 447.
- 15 A. Imhof and D. Pine, *Nature*, 1997, **389**, 948.
- 16 B. Holland, C. Blanford and A. Stein, *Science*, 1998, **281**, 538; J. Wijnhoven and W. Vos, *Science*, 1998, **281**, 802.
- 17 A. Zakhidov, R. Baughman, Z. Iqbal, C. Cui, I. Khayrullin, S. Dantas, J. Marti and V. Ralchenko, *Science*, 1998, **282**, 897.
- 18 O. Velev, P. Tessier, A. Lenhoff and E. Kaler, *Nature*, 1999, **401**, 548; Y. Vlasov, N. Yao and D. Norris, *Adv. Mater.*, 1999, **11**, 165.
- 19 A. Blanco, E. Chomski, S. Grabtchak, M. Ibisate, S. John, S. Leonard, C. Lopez, F. Meseguer, H. Miguez, J. Mondia, G. Ozin, O. Toader and H. Driel, *Nature*, 2000, **405**, 437.
- 20 Y. A. Vlasov, X. Bo, J. C. Sturm and D. J. Norris, *Nature*, 2001, **414**, 289.
- 21 M. Notomi, K. Yamada, A. Shinya, J. Takahashi, C. Takahashi and I. Yokohama, *Phys. Rev. Lett.*, 2001, **87**, 253902.
- 22 R. D. Meade, A. Devenyi, J. D. Joannopoulos, O. L. Alerhand, D. A. Smith and K. Kash, *J. Appl. Phys.*, 1994, **75**, 4753.
- 23 R. F. Cregan, B. J. Mangan, J. C. Knight, T. A. Birks, P. St. J. Russell, P. J. Roberts and D. C. Allan, *Science*, 1999, **285**, 1537.
- 24 W. Lee, S. Pruzinsky and P. Braun, *Adv. Mater.*, 2002, **14**, 271; T. Taton and D. Norris, *Nature*, 2002, **416**, 685.
- 25 Y. Ye, S. Badilescu and V.-V. Truong, *Appl. Phys. Lett.*, 2002, **81**, 616.
- 26 T. Parrill, *J. Mater. Res.*, 1992, **7**, 2230; R. Parrill, *J. Mater. Res.*, 1994, **9**, 723.
- 27 J. Aizenberg, P. V. Braun and P. Wiltzius, *Phys. Rev. Lett.*, 2000, **84**, 2997; Y. Ye, S. Badilescu, V. Truong, P. Rochon and A. Natansohn, *Appl. Phys. Lett.*, 2001, **79**, 872.
- 28 A. V. Blaaderen, R. Ruel and P. Wiltzius, *Nature*, 1997, **385**, 321.
- 29 Y. Yin, Y. Lu and Y. Xia, *J. Mater. Chem.*, 2001, **11**, 987.
- 30 A. D. Dinsmore, A. G. Yodh and D. J. Pine, *Nature*, 1996, **383**, 239; K. Lin, J. C. Crocker, V. Prasad, A. Schofield, D. A. Weitz, T. C. Lubensky and A. G. Yodh, *Phys. Rev. Lett.*, 2000, **85**, 1770.
- 31 S. M. Yang and G. A. Ozin, *Chem. Commun.*, 2000, **24**, 2507; S. Yang, H. Miguez and G. A. Ozin, *Adv. Funct. Mater.*, 2002, **12**, 425.